Int J Earth Sci (Geol Rundsch) (2006) 95: 529–541
DOI 10.1007/s00531-005-0042-x

ORIGINAL PAPER

Juliane Ramelow · Ulrich Riller · Rolf L. Romer
Onno Oncken

Kinematic link between episodic trapdoor collapse of the Negra Muerta Caldera and motion on the Olacapato-El Toro Fault Zone, southern central Andes

Received: 27 April 2004 / Accepted: 12 August 2005 / Published online: 6 October 2005
© Springer-Verlag 2005

Abstract A combined geochronological and structural analysis of the Miocene Negra Muerta Caldera was designed to better understand caldera formation associated with prominent faults on the central Andean plateau. Rb–Sr ages of the caldera outflow facies indicate that caldera formation occurred in two volcanotectonic episodes. The first episode commenced with explosive eruption of the 9.0 ± 0.1 Ma andesitic Acay Ignimbrite followed by a period of volcanic quiescence and moderate tectonic activity. Dominant volcanic and tectonic activity occurred during the second episode, which is bracketed by eruption of the 7.6 ± 0.1 Ma rhyolitic Toba 1 Ignimbrite and effusive discharge of the 7.3 ± 0.1 Ma rhyodacitic to andesitic lava flows. Structural relationships between rocks of the Negra Muerta Volcanic Complex and collapse-induced normal faults, notably NE-striking normal faults, agree with simultaneous volcanic activity and floor subsidence of the caldera during the second episode. Floor subsidence was achieved by tilting on an outward dipping reverse fault to the northwest of the caldera floor around a hinge zone located south of the caldera floor. This induced horizontal extension of the caldera floor and was accomplished by fragmentation of, and intrusion of dikes into, the floor. Collapse-induced and post-collapse fault populations of the caldera do not differ significantly in the directions of their axes of maximum extension and are in this respect kinematically compatible with left-lateral slip on the nearby Olacapato-El Toro Fault Zone. This furnishes evidence for a kinematic control by prominent faults on the formation of collapse calderas in the central Andes. The structural analysis of the Negra Muerta Caldera shows that collapse calderas can serve as deformation markers that contribute in elucidating the regional kinematic regime and the time of activity of prominent dislocations genetically related to collapse calderas.

Keywords Collaps caldera · Geochronology · Kinematics · Deformation · Central Andes

J. Ramelow · U. Riller (✉) · R. L. Romer · O. Oncken
GeoForschungsZentrum Potsdam, Telegrafenberg,
14473 Potsdam, Germany

U. Riller
Museum für Naturkunde, Institut für Mineralogie,
Humboldt-Universität zu Berlin, Invalidenstrasse 43,
10115 Berlin, Germany
E-mail: ulrich.riller@museum.hu-berlin.de
Tel.: +49-31-20938573
Fax: +49-31-20938565

Introduction

Unravelling the mechanism of collapse caldera formation is vital in understanding the relationship between magmatism and deformation at shallow crustal levels. Particularly in convergent orogenic belts, localised deformation is often invoked to drive formation of collapse calderas which are generally asymmetric in plan view (Bellier and Sébrier 1994; Ventura 1994; Moore and Kokelaar 1997; Acocella et al. 1999). Based on fault geometry, stratigraphic evidence and geometry of the caldera floor, the interface between rock masses collapsed into an underlying magma chamber and volcanic deposits, four end member collapse modes can be discerned (Fig. 1: Walker 1984; Lipman 1997). Plate or piston collapse is accomplished by subsidence of a relatively coherent caldera floor on one or several steeply dipping ring faults. By contrast, downsag subsidence is characterised by flexural inward tilting of wall rocks, whereby ring faults with large displacements are generally not developed. Trapdoor collapse involves asymmetric floor subsidence either by tilting around a linear hinge zone or differential block faulting whereby collapsed rock is confined by a partial ring fault. Vertical displacement of the caldera floor on this ring fault increases away from the hinge zone. Piecemeal collapse results in an apparently non-systematic fragmentation of the caldera floor and the underlying substrate into differentially subsiding blocks. Calderas formed by the plate or downsag collapse modes are likely to be sub-

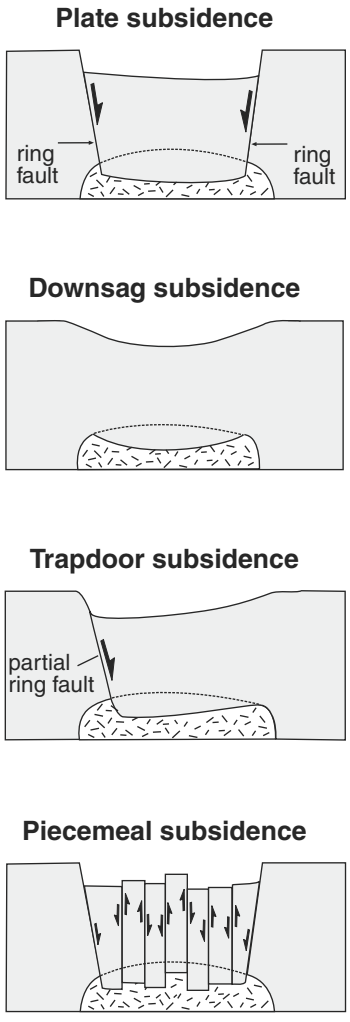

Fig. 1 Schematic illustration showing end member collapse modes (modified after Lipman 1997). For explanation see text

circular at surface whereas those generated by the trapdoor or piecemeal modes are often markedly asymmetric (Moore and Kokelaar 1997; Acocella et al. 1999). This may indicate that circular calderas formed as a consequence of magma overpressure whereas trapdoor and piecemeal modes are preferentially associated with localised deformation of the upper crust as a result of regional tectonism.

In the central Andes, Miocene to Pliocene volcanism affected large parts of the Puna, a high-altitude plateau confined to the west and east by the active magmatic arc and the eastern Cordillera, respectively (Fig. 2). Here, voluminous felsic ignimbrites erupted between about 10 and 1 Ma from collapse calderas which compose the Altiplano-Puna Volcanic Complex (de Silva 1989) and several NW-trending transverse volcanic belts (Viramonte and Petrinovic 1990). These volcanic belts are spatially associated with major fault zones, such as the Olacapato-El Toro Fault Zone (Fig. 2), a system of faults which has been intermittently active since the Paleozoic and which accomplished left-lateral displacement on the order of 20 km in Neogene time (Allmendinger et al. 1983). Orogen-parallel dilation on NW-striking fault zones generated by late Cenozoic differential crustal shortening may well have facilitated magma ascent and caldera formation in the Puna (Riller et al. 2001; Riller and Oncken 2003). Nonetheless, the genetic relationship between regional-scale, upper-crustal faulting and collapse caldera formation in the transverse volcanic belts remains to be ascertained. Identification of the collapse mechanism may be valuable in this respect. In the Puna, this is generally difficult to determine as the arid climate effectively prevents erosion of volcano-sedimentary deposits which generally obscure caldera floors and caldera-forming structures. To date, information on the mode of collapse exists only for the La Pacana caldera, located on the northwestern segment of the Olacapato-El Toro Fault Zone (Fig. 2). Based on the asymmetric distribution of erupted volcanic rocks and asymmetric subsidence of the caldera floor on a partial ring fault, formation of this resurgent caldera was likely initiated by trapdoor collapse (Lindsay et al. 1999).

Here, we report on a combined field-structural and geochronological analysis of the Negra Muerta Caldera (Fig. 3) which aims at constraining mode and history of its formation. This study is the first of its kind in the southern central Andes and pertains to better understand the relationship between upper-crustal tectonism and collapse-caldera formation in this region (J. Ramelow, unpublished data). The Negra Muerta Caldera is the easternmost collapse caldera of the Puna and located at the morphotectonic transition to the Eastern Cordillera (Fig. 2). It is asymmetric in plan view and morphologically characterised by a well-preserved northern and western topographic rim (Fig. 3a), the top of which is about 5,500 m above sea level (asl). In contrast, the southern and eastern margins of the caldera, as well as much of its interior, have been largely eroded due to Pleistocene glacial activity and strong headward fluvial incision by the Calchaquí River. As a consequence, the structural caldera floor is well exposed from about 4,700 m asl in the north to about 3,900 m asl in the south (Fig. 3a). Excellent exposure of collapse-related structures and subvolcanic rocks in the caldera centre furnishes ideal conditions to determine the collapse mode of the caldera. Using the Rb–Sr method, volcanic units of the outflow facies were dated to constrain distinct collapse pulses. Our study complements that by Petrinovic et al. (2005) who examined the Negra Muerta Caldera in terms of its magmatic evolution.

Geologic setting of the Negra Muerta Caldera

Collectively, Cretaceous and Tertiary sedimentary rocks of the Salta Group resting unconformably on low-grade metamorphic metapelite of the Cambrian Puncoviscana Formation form the substrate of the Negra Muerta Caldera (Fig. 3, 4a). The Salta Group formed during

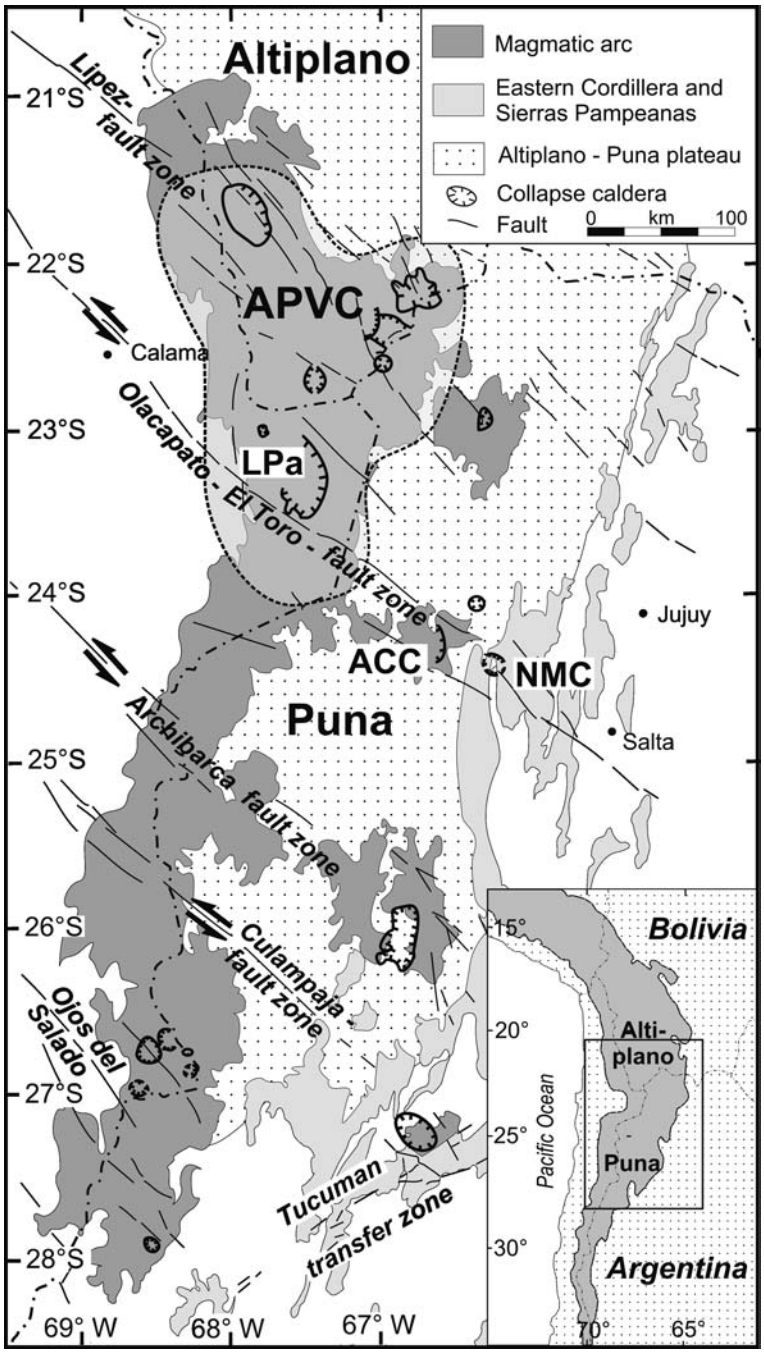

Fig. 2 Simplified map showing morphotectonic units and major NW-trending fault zones of the southern central Andes. Collapse calderas are spatially associated with these fault zones and define the NW-trending transverse volcanic belts and the Altiplano Puna Volcanic Complex (*APVC*). *ACC* Aguas Calientes Caldera, *NMC* Negra Muerta Caldera, *LPa* La Pacana Caldera

and after a phase of continental rifting in NW-Argentina and Bolivia that led to deposition of clastic sediments, mafic lava flows and carbonate rocks in distinct, but linked rift basins (Salfity and Marquillas 1994; Gonzalez-Bonorino et al. 1999). The 130–75 Ma Pirgua Subgroup forms syn-rift deposits and consists of ruby-coloured sandstone, conglomerate and intercalated basalt flows (Vilela 1951; Reyes and Salfity 1973). In the caldera centre, these rocks are about 40–50-m thick and overlain by the 75–73 Ma Lecho Formation, a 10–20-m thick unit consisting of white calcareous conglomerate and sandstone. Dolomite and limestone of the 73–63 Ma Yacoraite Formation are up to 50 m thick in the caldera and considered as initial post-rift deposits. The formation is characterised by grey stromatolite and cream-coloured to black oolite layers intercalated with yellow limestone beds (Turner 1959). The Lecho and Yacoraite Formations make up the Balbuena Subgroup (Fig. 4a). The upper Salta Group consists again of clastic sedimentary rocks, specifically the 63–54 Ma Mealla and the 54–49 Ma Maiz Gordo Formations (Moreno 1970; Del Papa 1999). The Mealla Formation comprises orange to purple-coloured sandstone beds separated by up to 2-m thick mud stone layers. By contrast, the Maiz Gordo Formation is characterised by about 70-m thick, fine-grained conglomerate rich in quartz clasts.

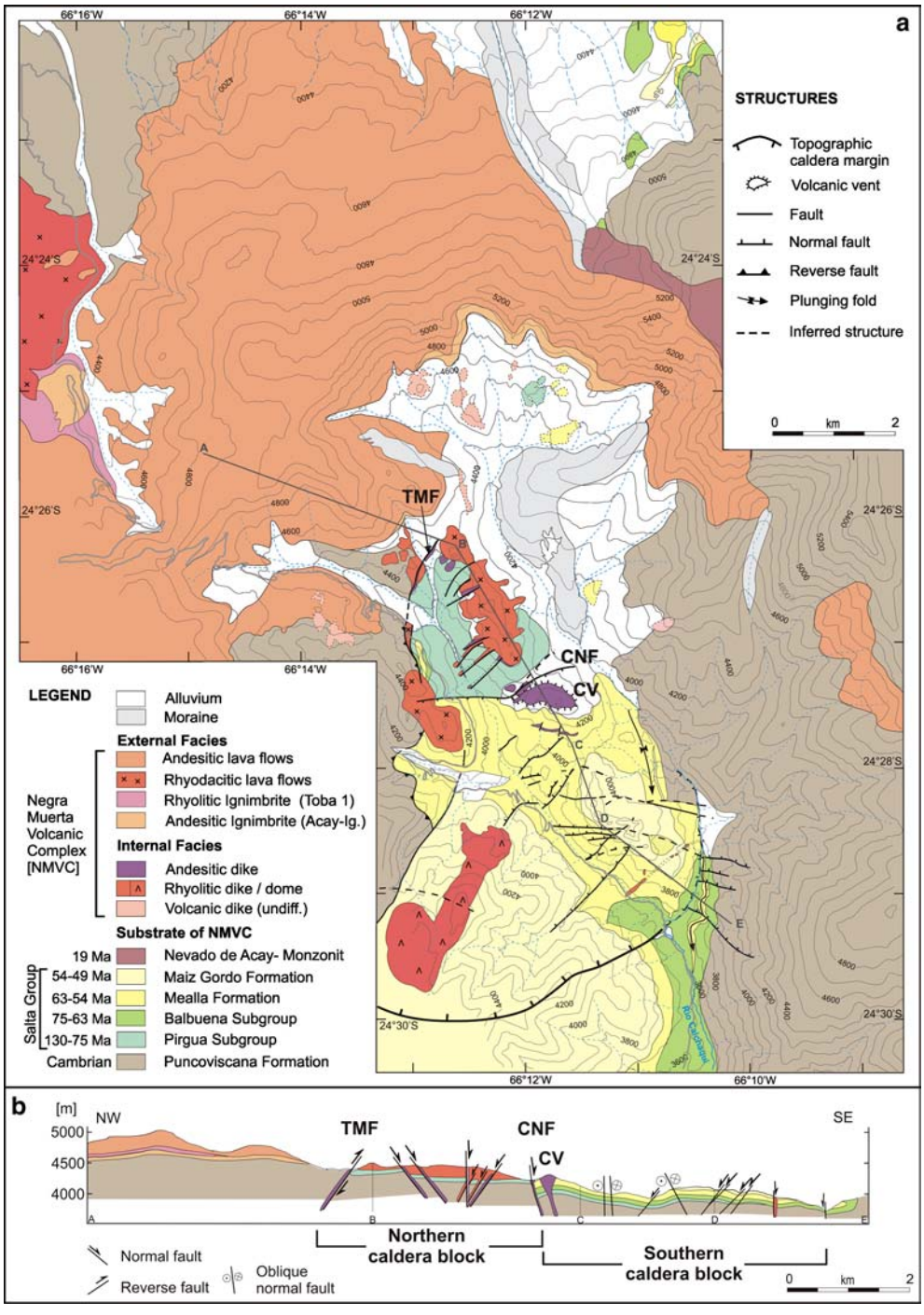

Fig. 3 Geological units and structure of the Negra Muerta Caldera. *TMF* Toro Muerto Fault, *CNF* Central Normal Fault, *CV* Central vent. **a** Geological map of the Negra Muerta Caldera modified from J. Ramelow, unpublished data. Line with node points A–E represents the trace of the profile shown in (**b**). **b** Profile through the Negra Muerta Caldera

E–W crustal shortening affected much of the central Andes during the Neogene (Isacks 1988; Allmendinger et al. 1997) and led to formation of major orogen-parallel reverse faults and folds as well as reactivation of pre-Neogene NW-striking structural discontinuities (Riller et al. 2001). In the Calchaquí Valley, such shortening is apparent from reverse faults at the valley margins that placed rocks of the Puncoviscana Formation over those of the Salta Group (Servicio Geológico Minero Argentina 1996). In the Negra Muerta Caldera, however, only the reverse fault at the western flank of the valley, the Toro Muerto Fault (Fig. 3a, b), is apparent, whereas at the eastern valley flank the contact between the Puncoviscana and the Lecho Formations is overturned but unstrained (Riller et al. 1999). This indicates that Late Cenozoic E–W shortening in the Negra Muerta area was chiefly accomplished by kilometre-scale folding of the Puncoviscana Formation and its Cretaceous-Tertiary cover rocks. Large-scale folding terminated probably prior to emplacement of the 19 Ma Nevado de Acay Pluton (Petrinovic et al. 1999), an unstrained monzonite body that intruded the Puncoviscana

and Yacoraite Formations at the northeastern portion of the caldera (Llambias et al. 1985). NW-striking faults of the Olacapato-El Toro Fault Zone are located at a distance of about 5 km to the north and south of the caldera and are kinematically linked with orogen-parallel folds (Allmendinger et al. 1983; Marrett et al. 1994; Riller et al. 1999, 2001). Field-structural evidence and seismic activity indicate that one of these faults to the north of the caldera, the Chorrillos Fault, has been active since Quaternary times (Marrett et al. 1994; Schurr et al. 1999).

Volcanic units of the Negra Muerta Caldera

Andesitic to rhyodacitic volcanic rocks erupted from the Negra Muerta Caldera are known as the Negra Muerta Volcanic Complex (Llambias et al. 1985; Petrinovic et al. 2005). The outflow facies of this complex consists of ash flow deposits and lava flows, whereas subvolcanic dikes and domes as well as relics of ash flow deposits and lava flows, make up the intra-caldera facies (Fig. 3a). The outflow facies is well preserved to the north and west of the caldera centre and consists of two ignimbrites, the andesitic Acay and the rhyolitic Toba 1 Ignimbrites, as well as rhyolitic and andesitic lava flows (Fig. 4b). The Acay Ignimbrite, a greenish tuff, covers the substrate of the caldera unconformably. The thickness of this ignimbrite varies between 100 and 150 m close to the caldera, but decreases with distance from the caldera. The ignimbrite is nonwelded at its base, strongly-welded and fiamme-rich in the middle part and again nonwelded in the uppermost 30–50 m. The mineral assemblage of the ignimbrite consists of plagioclase, alkali feldspar, biotite, green hornblende and corroded quartz, all of which display flow banding. Point counting of thin sections indicates that the pumice contains about 15–30% crystals. The matrix of the ignimbrite is poor in lithic fragments (6%), but rich in phenocrysts (up to 35%), which may point to high viscosity during eruption of this melt.

The Acay Ignimbrite is covered by the Toba 1 Ignimbrite (Viramonte et al. 1984; Petrinovic et al. 1999, 2005), a homogeneous and nonwelded rhyolitic ash flow deposit (Fig. 4b). This ignimbrite occurs as a coherent 30–50-m thick unit chiefly to the NW of the caldera (Fig. 3a) and is characterised by crystal-rich pumice (30–45%), lithic fragments, and phenocrysts of quartz and plagioclase (up to 60%). Plagioclase laths are up to 2-cm long and randomly distributed in a white glass matrix. Based on colour, two pumice variants can be discerned in the ignimbrite, a dark-grey and a cream-coloured one. Both variants are similar in their phenocryst content, that is 70% feldspar, 21% quartz and about 8% biotite. In places, however, the dark-grey variant may contain up to 20% biotite phenocrysts.

The Toba 1 Ignimbrite is overlain by distinctive 10–20-m thick glassy-porous to massive rhyodacitic lava flows (Fig. 4b). These are rich in plagioclase, alkali feldspar, biotite and quartz phenocrysts. Locally, the rhyodacitic lava flows are autobrecciated, probably as a consequence of lava dome collapse. The top of the outflow facies consists of up to 300-m thick, monotonous andesitic lava flows, which cover an area of approximately 105 km^2 (Fig. 3a).

Except for some relics of ashflow deposits and lava flows, volcanic rocks have been eroded in the caldera centre (Fig. 3a). Consequently, subvolcanic equivalents to the outflow deposits, specifically rhyodacitic and andesitic dikes and vents that intruded the sedimentary substrate of the caldera are exposed in the caldera centre and characterise the intra-caldera facies (Fig. 3a). Rhyodacitic rocks contain up to 65% plagioclase, alkali feldspar, rounded quartz and sub- to euhedral biotite phenocrysts set in a matrix of microlitic feldspar and rhyolitic glass. Similarly, phenocrysts of andesites contribute to more than 50% of the whole rock, whereby the mineral assemblage consists of plagioclase, alkali feldspar, rounded quartz, biotite, hornblende and augite. Subvolcanic rocks are often hydrothermally altered. Rhyodacitic dikes forming the feeder system to overlying lava flows in the centre of the caldera and a large elongate rhyodacitic dome at the southern portion of the caldera strike NE–SW. By contrast, 10–20-m thick, NE-striking andesitic dikes in the caldera centre truncate rhyodacitic dikes (Fig. 3a). This indicates that andesitic dikes formed after rhyodacitic ones and is in agreement with the stratigraphy of the outflow facies (Fig. 4b).

Rb/Sr-geochronology

The Negra Muerta Volcanic Complex has been affected to varying degrees by post-magmatic alteration. Rock samples from the outflow facies are only slightly altered whereas the dikes and vents of the intra-caldera facies underwent a significant hydrothermal activity. We therefore limited the radiometric age determination to pumice samples of the Acay and Toba 1 Ignimbrites and a specimen of an andesitic lava flow. To further minimise the disturbance of the geochemical system of the volcanic rocks by any alteration and contamination from the country rock we obtained radiometric ages using separates of biotite, feldspar and apatite. Separates were analysed using the Rb–Sr method at the GeoForschungsZentrum Potsdam.

The analytical procedures and the results are summarised in Table 1. The data are shown in Fig. 5. Since apatite may be affected by post-crystallisation uptake of Sr, all reported ages represent feldspar-biotite two-point ages. For the Acay Ignimbrite we obtained an age of 9.0 ± 0.1 Ma (2σ), whereas the overlying Toba 1 Ignimbrite gave an age of 7.6 ± 0.1 Ma (2σ). This age of the Toba 1 Ignimbrite corresponds well with a K–Ar age of 7.4 ± 0.1 Ma (2σ) determined by Petrinovic et al. (1999) for a whole rock sample of the same ignimbrite. The sample of the andesitic lava flow yielded an age of

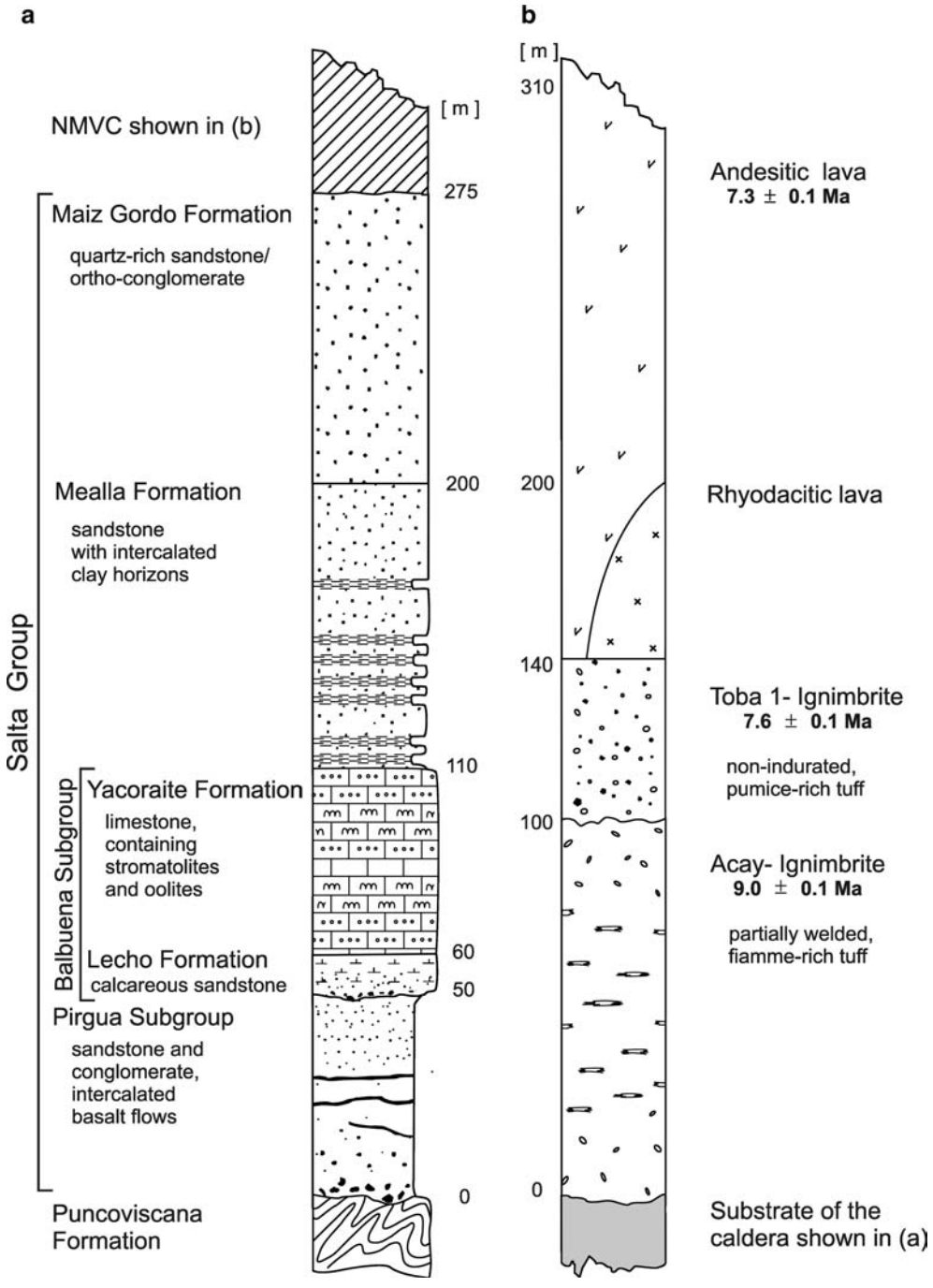

Fig. 4 Stratigraphy of the Negra Muerta Volcanic Complex and its substrate. **a** Stratigraphy of the Paleozoic to Tertiary substrate of the Negra Muerta Volcanic Complex (NMVC). **b** Stratigraphic profile of the outflow facies of the Negra Muerta Volcanic Complex. Rb–Sr ages of individual units of the complex from this study are indicated (see Fig. 5)

7.3 ± 0.1 Ma (2σ) indicating that magmatic activity continued after the climactic eruption. The ages obtained in this study are consistent with stratigraphy (Fig. 4). Due to the lack of exposure of specimens suitable for radiometric dating, there are no age data on rhyodacitic lava flows. Based on stratigraphical evidence, however, we expect, that the rhyodacitic lava flows extruded after the formation of the Toba 1 Ignimbrite and prior to emplacement of andesitic lava flows. Thus, their age can be restricted to between 7.6 and 7.3 Ma.

Structure and mode of floor subsidence of the Negra Muerta Caldera

Knowledge of the fault pattern generated as a consequence of caldera formation is paramount to assess the mode and history of collapse. Collapse-induced discontinuities of the Negra Muerta Caldera are well apparent in the partially-eroded caldera floor by the presence of displaced lithological contacts in distinct sedimentary marker beds such as stromatolite, sandstone and

Table 1 Rb–Sr data for three units of the volcanic sequence

Sample	Sample weight (mg)	Rb (ppm)	Sr (ppm)	$^{87}Rb/^{86}Sr^{a}$	$^{87}Sr/^{86}Sr^{b}$	Age (Ma)
NM-82						
Acay- apa	0.74	2.68	519.0	0.015	0.710122 ± 21	
Acay- fsp	7.81	32.9	1050.0	0.090	0.710159 ± 21	
Acay- bio	1.0	723.0	33.8	62.0	0.718062 ± 47	9.0 ± 0.1
NM-5						
Toba 1- apa	1.87	1.50	396.0	0.011	0.707900 ± 13	
Toba 1- fsp	4.63	13.4	1310.0	0.030	0.707542 ± 16	
Toba 1- bio	1.0	1520.0	15.2	290.0	0.738829 ± 79	7.6 ± 0.1
NM-74						
Lava-apa	0.5	1.44	458.0	0.009	0.710140 ± 62	
Lava-fsp	4.92	7.11	1190.0	0.017	0.710322 ± 17	
Lava-bio	2.47	440.0	22.9	55.6	0.716110 ± 43	7.3 ± 0.1

Rb and Sr concentrations were determined by isotope dilution using a ^{84}Sr–^{87}Rb-Spikes. Rb and Sr were seperated using standard ion-exchange procedures (Bio Rad AG50-X8 and 2.5 N HCl medium);
[a] 2σ error = 1%
[b] errors are $2\sigma_m$ and refer to the last two digits; $^{87}Sr/^{86}Sr$ normalized using $^{86}Sr/^{88}Sr = 0.1194$. During the measurement period NBS 987 strontium reference material gave $^{87}Sr/^{86}Sr = 0.710255 \pm 10$ ($n = 4$).

conglomerate layers of the Salta Group (Figs. 3a, 4a, 6). The correlation of displaced stratigraphic units across discontinuities allowed us to estimate displacement magnitudes (see below), as well as the kinematics of prominent collapse-induced discontinuities. The discontinuities consist generally of planar to sinuous NE- to E-striking normal faults that affected also relics of intra-caldera volcanic rocks (Fig. 3b). A coherent ring fault is not apparent in the Negra Muerta Caldera.

The Toro Muerto Fault is one of the most prominent discontinuities of the Negra Muerta Caldera and is located in the west-central portion of the caldera (Fig. 3a). As mentioned already, motion on this west-dipping reverse fault commenced prior to formation of the caldera. However, in the northern segment of the fault, rocks of the Cambrian Puncoviscana Formation are juxtaposed against rhyodacitic lava flows. North of this locality, the fault strike changes from N–S to NE–SW and here, an andesitic dike intruded into the fault zone. This suggests that the Toro Muerto Fault acted as a reverse fault during caldera formation. A second collapse-induced master fault is the south-dipping Central Normal Fault

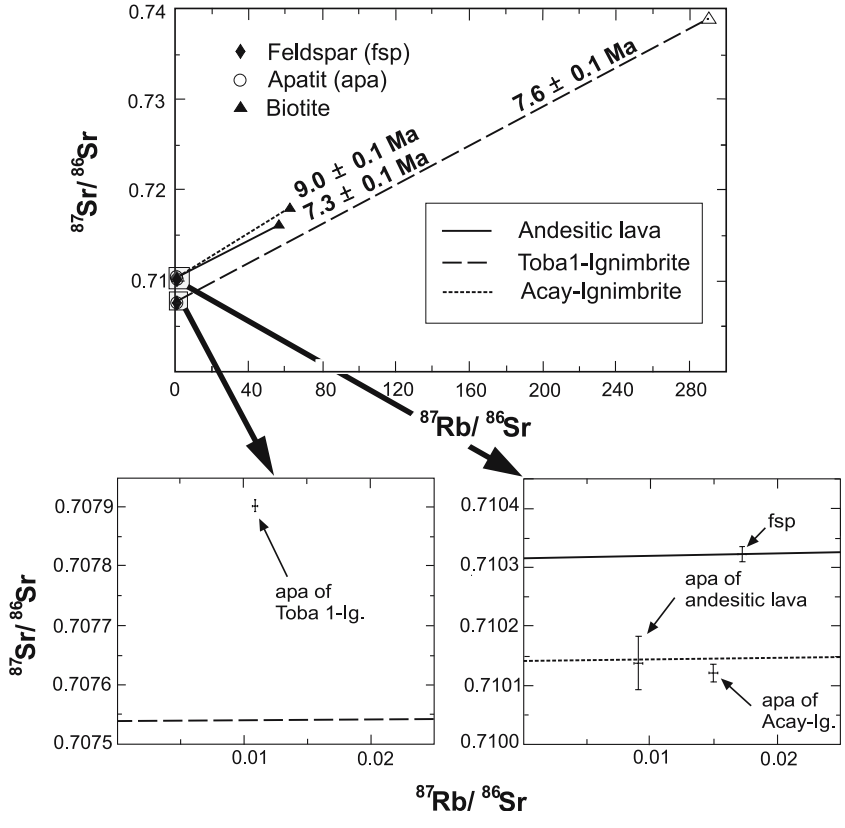

Fig. 5 Rb–Sr isochrons for the Acay and the Toba 1 Ignimbrites and an andesitic lava flow. Ages of the volcanic units are calculated using feldspar and biotite. Apatite does not fall within error limits on the regression line defined by the feldspar and biotite pairs, which may reflect post-crystallization uptake of vagabonding radiogenic Sr through apatite, especially in the porous samples of the Toba 1 pumice and the andesitic lava flow. The consideration of the apatite data would have no significant influence on the calculated ages

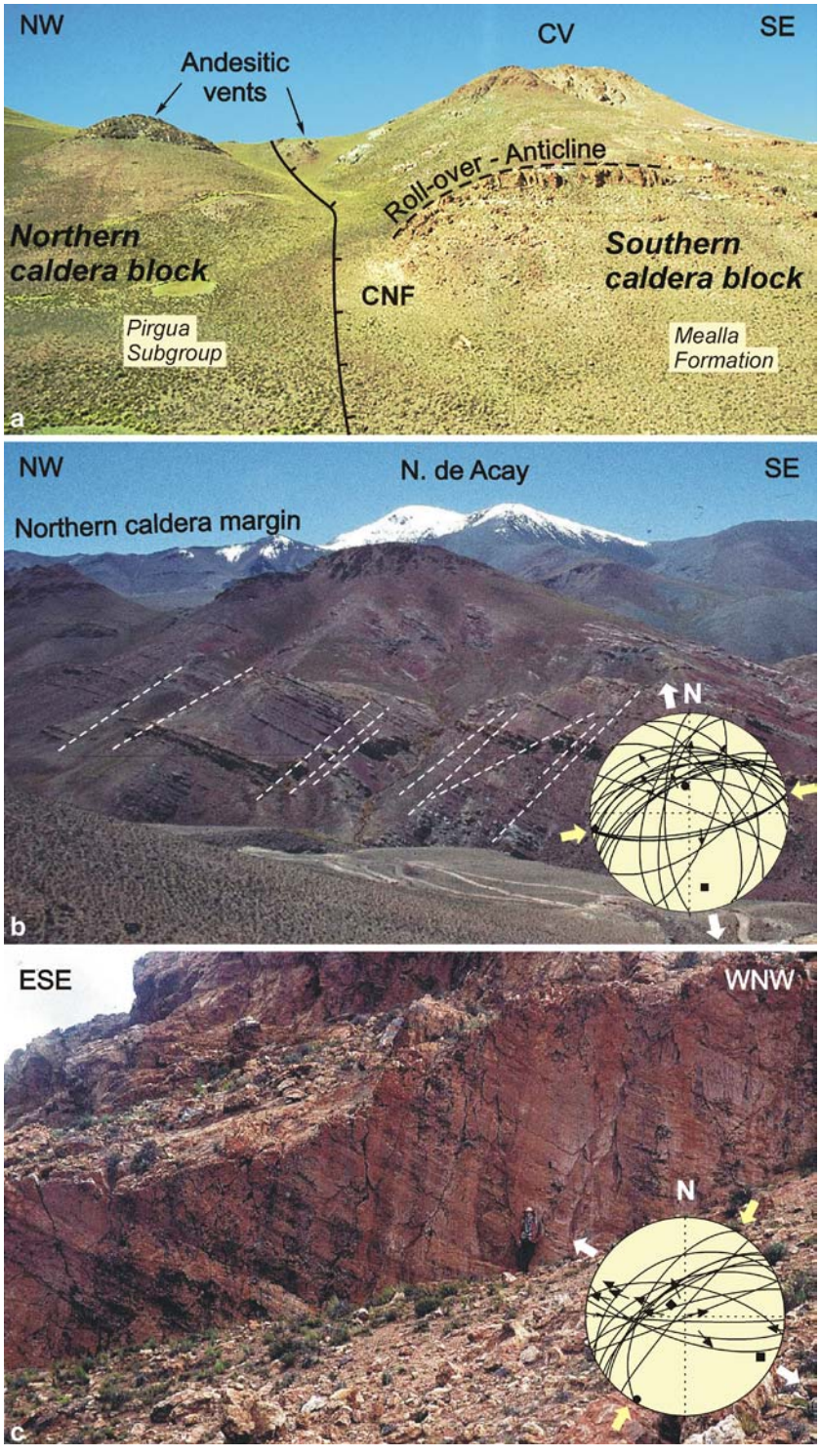

Fig. 6 Photographs showing structural field relationships and location of vents in the Negra Muerta Caldera. **a** The central normal fault (*CNF*) in the caldera centre bisects the caldera floor into a northern and a southern caldera block, evident from juxtaposition of the Pirgua Subgroup and the Mealla Formation. Note the roll-over anticline and the central vent (*CV*) in the hanging wall of the normal fault. **b** System of NW-dipping normal faults (*stippled lines*) in the southern caldera block displacing distinct sandstone and conglomerate beds of the Mealla Formation. **c** Displacement of the topographic surface by a post-collapse left-lateral, oblique-normal fault in the southern caldera block. Note the well-developed striae on fault surface and person for scale. Insets in (**b**) and (**c**) show lower-hemisphere, equal-area projections of the respective population of faults (*great circles*) and senses of slip on their surfaces (*arrows*). Horizontal components of shortening (*yellow arrows*) and extension (*white arrows*) are inferred from the P–T method (Turner 1953)

(Fig. 3). Based on the distribution of Tertiary rocks in the caldera substrate, this fault divides the caldera floor into a northern and a southern caldera block (Fig. 3b). More specifically, the top of the northern block is made up of sedimentary rocks of the Cretaceous Pirgua Subgroup, whereas the youngest pre-caldera rocks of the southern block consist of the Eocene Maiz Gordo Formation. Juxtaposition of Upper Cretaceous rocks of the Pirgua Subgroup against rocks of the Tertiary Mealla Formation (Figs. 3, 6a) indicates a vertical offset between the two blocks of at least 150 m at the Central Normal Fault. The presence of a roll-over anticline in the sedimentary strata of the hanging wall, that is the northern portion of the southern block (Fig. 6a), suggests that the fault has a listric geometry (e.g. Wernicke and Burchfiel 1982). Andesitic volcanic vents and

numerous quartz veins are spatially associated with the hinge zone of this anticline and the Central Normal Fault. Thus, ascent and eruption of andesite may have been facilitated, if not triggered, by local dilation due to folding and faulting of the caldera floor.

Both caldera blocks are distorted by second-order, NE-striking faults, which dip either to the SE or NW, and subvertical ENE-striking faults (Figs. 3, 7). NE-striking faults show normal sense of displacement and are characterised by up to 0.5-m thick quartzitic fault breccias, fault striae and strong hydrothermal alteration. Subvolcanic dikes are generally concordant to, or emplaced into, the normal fault zones. This is typical of concurrent tectonic and magmatic activity. Displaced stratigraphic marker beds (Fig. 6b) indicate that the magnitude of vertical displacement on these normal faults varies between 10 and 70 m, whereby displacement magnitudes decrease generally towards the southern margin of the caldera (Fig. 7b). This gradient in finite vertical displacement and the apparent absence of a coherent ring fault suggests that the Negra Muerta caldera formed by asymmetric floor subsidence around a hinge zone located to the south of the caldera (Fig. 7c). However, differential vertical displacement on second-order normal faults in both blocks (Fig. 7a) also points to fragmentation of the caldera floor, indicative of piecemeal floor subsidence (Fig. 1). The cumulative vertical displacement of all collapse-related normal faults, including the Central Normal Fault, amounts to 450 m. Based on the average inclination of 50° of the normal faults (Fig. 3b), this translates to a minimum of about 380 m of horizontal NW-SE extension of the caldera floor in addition to dilation by dike emplacement. This extension corresponds well to the length change (ΔL in Fig. 7c) of the caldera floor, predicted for asymmetric floor subsidence along the NW-dipping Toro Muerto Fault around a hinge zone located to the south of the Negra Muerta Caldera (Fig. 7a, c). Thus, the Toro Muerto Fault may be part of a partial ring fault system, the eastern portion of which is obscured by Quaternary deposits in the caldera (Fig. 3a). This simple model of caldera formation suggests that fragmentation of the caldera floor by normal faulting is intrinsic to asymmetric floor subsidence along a reverse fault that is located opposite to, and dips away from, the hinge.

Vertical displacement on second-order normal faults and consequently horizontal extension is larger in the northern block than it is in the southern block (Fig. 7b).

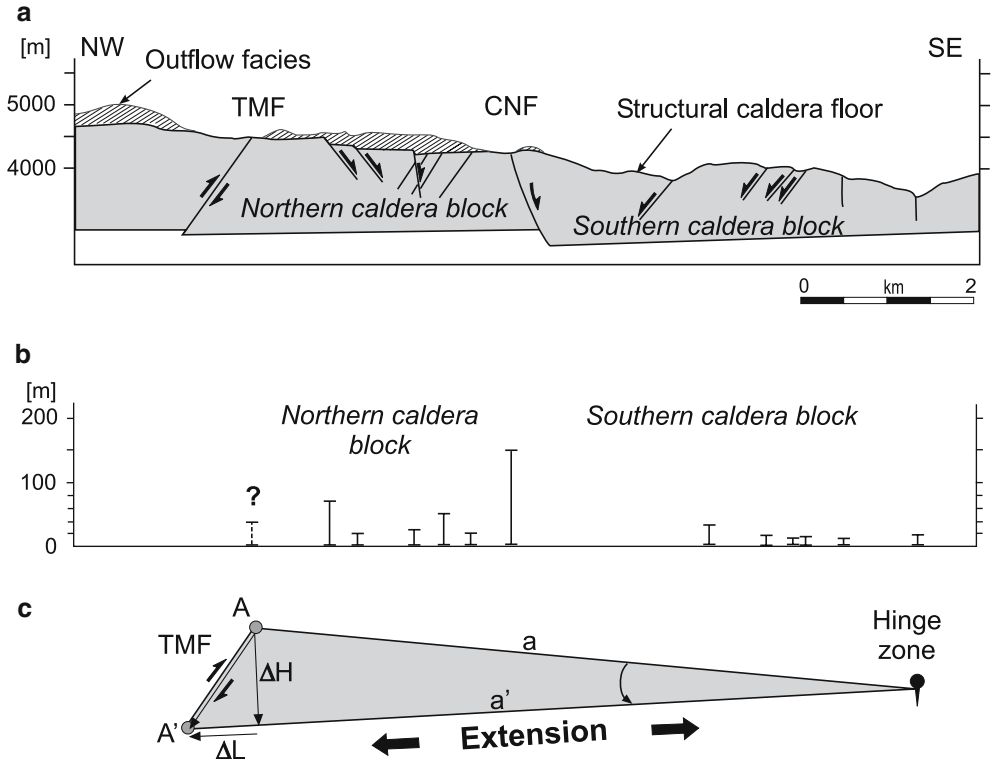

Fig. 7 Subsidence of the Negra Muerta Caldera floor. **a** NW–SE profile of the Negra Muerta Caldera showing prominent collapse-induced faults and the partially-exposed structural caldera floor. The TMF and the CNF define the northern caldera block. The CNF to the north and the partially eroded topographic margin to the south confine the southern caldera block. **b** Diagram showing the vertical displacement magnitudes for prominent faults inferred from offset stratigraphic markers with respect to position on the NW–SE profile in (**a**). Note the differences in magnitudes between the northern and southern caldera floors. **c** Model showing caldera formation by asymmetric subsidence on the TMF around a hinge zone and fragmentation of the caldera floor. The displacement of a point A to the position A′ on the TMF is accomplished by the components of subsidence (ΔH) and horizontal extension (ΔL), whereby ΔL is the difference in pre-collapse (a) and post-collapse length (a') of the caldera floor. Horizontal extension is accommodated by normal faulting and dike intrusion which lead to fragmentation of the caldera floor

This correlates with the apparent volume of subvolcanic dikes emplaced into the normal faults. More specifically, the thickness and density of dikes in the northern block are much higher than in the southern block (Fig. 3). This suggests that dike emplacement and eruption of volcanic rocks is controlled by horizontal extension and underscores the notion of simultaneous magmatic and tectonic activity, i.e. caldera floor subsidence.

NE-striking normal faults, subvolcanic dikes, as well as the rhyodacitic dome, are cut by steeply-dipping, ENE-striking faults (Figs. 3a, 6c). These faults are characterised by grooves and striations, the orientation of which indicate left-lateral oblique normal sense of displacement on the faults. The apparent horizontal offset of lithological boundaries by these faults is up to 700 m (Fig. 3a). The component of vertical displacement evident from fault scarps that displaced the topographic surface is often on the order of 10–15 m (Fig. 6c). This indicates that ENE-striking faults postdate caldera formation and have been active most probably up to Quaternary times or even recently.

To elucidate collapse-induced and post-collapse deformation, both fault populations were analysed in terms of their kinematic axes using the P–T method. This method is based on knowledge of fault orientations, directions and senses of slip on the fault surfaces of a given fault population (Turner 1953). The faults and principal kinematic axes for collapse-induced normal faults and Quaternary to Recent oblique-normal faults are depicted in the stereographic projections in Fig. 6b, c, respectively. The diagrams show that the directions of horizontal extension for both fault populations differ by about 30°. Thus, syn-collapse and post-collapse deformation in the Negra Muerta Caldera did not vary significantly in terms of these kinematic axes. Components of approximately NE–SW shortening and NW–SE extension are apparent in both fault populations. This is kinematically compatible with left-lateral slip on the ENE-striking Olacapato-El Toro Fault Zone (Fig. 2). Such kinematic compatibility between collapse-induced structures and regional faults, as well as evidence for syntectonic eruption of the Negra Muerta Volcanic Complex, suggests that localised upper-crustal deformation drove ascent and eruption of viscous magma and possibly asymmetric collapse of this caldera.

Collapse history of the Negra Muerta Caldera

Estimates of the displacement magnitudes on collapse-related faults, their structural relationship to rocks of the Negra Muerta Volcanic Complex and the radiometric ages of this complex allows us to crudely reconstruct the collapse history of the Negra Muerta Caldera (Fig. 8). The reconstruction is based on the fact that large-scale folding of Paleozoic to Eocene (meta)-sedimentary rocks terminated prior to the onset of caldera formation, as strata of the Negra Muerta Volcanic Complex were not affected by the folding. However, the reconstruction is based on the assumption that Tertiary strata were continuously present in the caldera at the onset of floor subsidence. This is supported by the presence of Tertiary rocks to the north and south of the caldera.

The first pulse of caldera formation occurred upon eruption of the 9.0 Ma Acay Ignimbrite (Fig. 8a). Based on the asymmetric distribution of this ignimbrite, this is its preferred occurrence to the northwest of the caldera (Fig. 3a), we speculate that it erupted along SE-dipping discontinuities such as the Central Normal Fault. This fault may well have been active during eruption of the Acay Ignimbrite and during the following period of volcanic quiescence. This is evident from the lack of Tertiary rocks in the northern caldera block but their presence in the southern block. Subsidence of the southern caldera block on the Central Normal Fault must have left the northern block at a higher topographic level and thus, more susceptible to erosion than the southern block. As a consequence, headward fluvial incision by the Calchaquí River (Fig. 8b) exposed the Cretaceous Pirgua Subgroup prior to emplacement of rhyodacitic lava flows on top of these rocks in the northern block (Fig. 8c). Fluvial erosion following the eruption of the Acay Ignimbrite also accounts for its general absence in the caldera.

The second volcano-tectonic pulse (Fig. 8c, d) is bracketed by the explosive eruption of the Toba 1 Ignimbrite at 7.6 Ma (episode 1) and effusive discharge of andesite at 7.3 Ma (episode 2). Assuming that the rhyodacitic lava flows are cogenetic with the 7.6 Ma Toba 1 Ignimbrite, the period of magmatic quiescence between the first and second volcano-tectonic pulses lasted approximately 1.4 Ma. The close spatial association of subvolcanic rhyodacitic and andesitic dikes with normal faults suggests that the majority of normal faults were active during the second volcano-tectonic pulse. This is corroborated by the displacement of rhyodacitic lava flows by normal faults, notably the Central Normal Fault (Fig. 3b), in the northern caldera block (Fig. 8d). Repeated activity of this fault during the second pulse led to formation of a roll-over anticline (Fig. 8d) and ascent of andesite at the central vent (CV in Fig. 8d) in its hanging wall. Emplacement of andesite into, and juxtaposition of the Puncoviscana Formation against rhyodacitic lava flows along, the Toro Muerto Fault indicates activity of this reverse fault during the second volcano-tectonic pulse. These relationships suggest that horizontal extension and asymmetric floor subsidence on the Toro Muerto Fault was most effective during the second volcano-tectonic pulse. Following this pulse, ESE-striking oblique-normal faults affected chiefly the southern portion of the Negra Muerta Caldera (Fig. 8e).

Geodynamic significance of collapse caldera formation

The structural analysis of the Negra Muerta Caldera points to kinematic compatibility between collapse-induced faults and the Olacapato-El Toro Fault Zone.

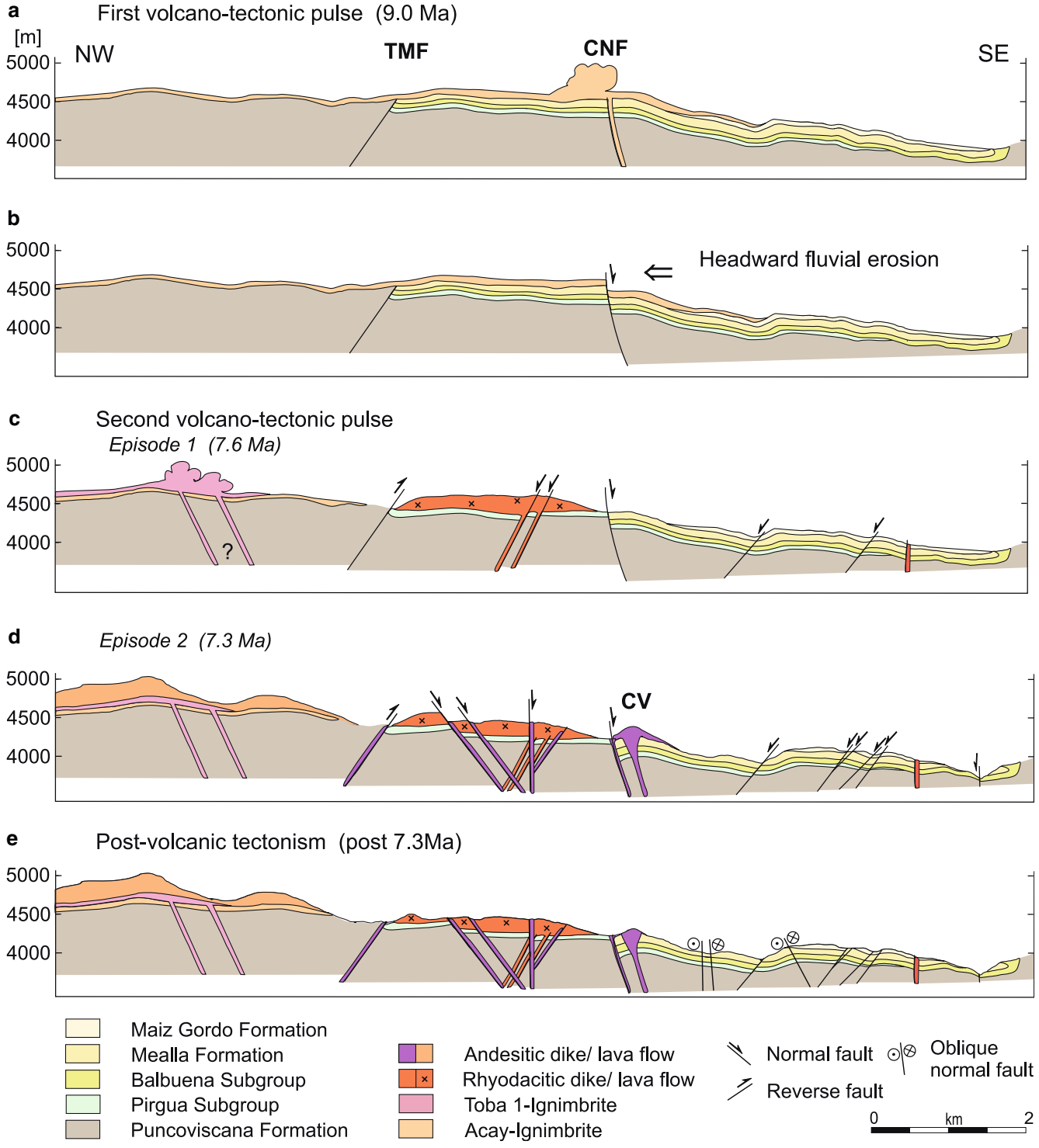

Fig. 8 Stages of collapse formation of the Negra Muerta Caldera. *CV* central vent, *TMF* Toro Muerto Reverse Fault, *CNF* central normal fault. For explanation of individual stages, see text

This supports the hypothesis that collapse-caldera formation and localised, upper-crustal deformation in the transverse volcanic belts are genetically related (Riller et al. 2001; Riller and Oncken 2003). A similar relationship between regional tectonism and mode of caldera formation has been invoked for the La Pacana Caldera (Lindsay et al. 1999) and the Aguas Calientes Caldera (Petrinovic et al. 1999), both located on the Olacapato-El Toro Fault Zone as well (Fig. 2). In fact, these calderas share conspicuous structural characteristics with the Negra Muerta including (1) asymmetric shape at surface, whereby the maximum caldera

diameter trends N–S, (2) asymmetric distribution of the outflow facies and (3) presence of a partial ring fault that likely accomplished asymmetric subsidence of the caldera floor. It is, therefore, conceivable that the La Pacana and the Aguas Calientes Caleras formed also by trap-door collapse and that this mechanism is typical for collapse caldera formation associated with the activity of major upper-crustal dislocations during regional tectonism.

Structural analysis of the Negra Muerta Caldera suggests also that collapse calderas may serve as giant deformation markers, that help to unravel not only the kinematic regime but also the time of activity of prominent dislocations associated with a collapse caldera. Thus, the Olacapato-El Toro Fault Zone was active in late Miocene times. South of this fault zone, Neogene volcanic activity is also related to a prominent NW–SE striking discontinuity, the Archibarca Fault Zone (Fig. 2: Richards and Villeneuve 2002). Late Miocene activity of NW–SE striking fault zones seems to have been an important characteristic of upper-crustal deformation in the central Andes, collapse caldera formation and concurrent felsic volcanism. North-south stretching of crust is indicated by the deformation regime in which the Negra Muerta Caldera and, by inference, the La Pacana and Aguas Calientes Calderas, formed by left-lateral slip on NW–SE striking dislocations. Such orogen-parallel stretching of upper crust may have been induced by changes in the deformation regime, i.e. from vertical crustal thickening to orogen-parallel extension (Riller et al. 2001; Caffe et al. 2002) or by the along-strike gradient in horizontal crustal shortening (Riller and Oncken 2003).

Conclusions

Age determination using the Rb-Sr method indicates that formation of the Negra Muerta Caldera occurred in two volcano-tectonic episodes. The first episode commenced with the eruption of the andesitic Acay Ignimbrite at 9.0 Ma followed by a period of volcanic quiescence and moderate tectonic activity that lasted about 1.4 million years. In contrast, principal volcano-tectonic activity occurred during the rather short second episode bracketed by the eruption of the 7.6 Ma rhyolitic Toba 1 Ignimbrite and the emplacement of 7.3 Ma andesitic lava flows. Simultaneous volcanic activity and subsidence of the caldera floor during this episode is evident from the (1) emplacement of subvolcanic dikes into collapse-induced normal faults, (2) correlation between volume of subvolcanic dikes and horizontal extension accomplished on these normal faults, (3) fault-controlled position of the central vent and (4) ascent and eruption of crystal-rich, viscous andesitic and rhyolitic ignimbrites and rhyodacitic lava flows. The pattern of collapse-induced normal faults indicates horizontal NW–SE to N–S extension, which fits a simple collapse model involving asymmetric subsidence of a fragmented caldera floor. The direction of maximum extension did not change significantly during post-collapse deformation and is kinematically compatible with left-lateral displacement on the nearby Olacapato-El Toro Fault Zone. This is in agreement with other recent studies linking caldera formation and associated localised volcanism to the activity of prominent NW-striking fault zones in the central Andes. The structural analysis of the Negra Muerta Caldera shows also that collapse calderas can serve as giant deformation markers that contribute in elucidating the kinematic regime and the time of activity of prominent dislocations genetically related to collapse calderas.

Acknowledgements This work was funded by the German Science Foundation (projects Ri 916/1-1, Ri 916/1-2 and subproject C1C of the collaborative research project SFB 267). We thank our colleagues at the Universidad Nacional de Salta, notably Ivan Petrinovic, Ricardo Alonso, José Viramonte and Fernando Hongn for scientific advice and logistical support. We acknowledge comments by O. Bellier and S. deSilva on an earlier version of the manuscript as well as a review for the Journal by an anonymous person.

References

Acocella V, Salvini F, Funiciello R, Faccenna C (1999) The role of transfer structures on volcanic activity at Campi Flegrei (Southern Italy). J Volcanol Geotherm Res 91:123–139

Allmendinger RW, Jordan TE, Kay SM, Isacks BL (1997) The evolution of the Altiplano-Puna Plateau of the Central Andes. Ann Rev Earth Plan Sci 25:139–174

Allmendinger RW, Ramos VA, Jordan TE, Palma M, Isacks BL (1983) Paleogeography and Andean structural geometry, Northwest Argentina. Tectonics 2:1–16

Bellier O, Sébrier M (1994) Relationship between tectonism and volcanism along the Great Sumatran fault zone deduced by SPOT image analyses. Tectonophysics 233:215–231

Caffe PJ, Trumbull RB, Coira BL, Romer RL (2002) Petrogenesis of early Neogene magmatism in the northern Puna; implications for magma genesis and crustal processes in the central Andean plateau. J Petrol 43:907–942

Del Papa CE (1999) Sedimentation on a ramp type lake margin; paleocene–eocene Maiz-Gordo formation, northwestern Argentina. J South Am Earth Sci 12:389–400

de Silva S.L (1989) Altiplano-Puna volcanic complex of the central Andes. Geology 17:1102–1106

Gonzalez Bonorino G, Omarini R, Viramonte J (1999) Geologia del Noroeste Argentino. XIV. Congreso Geológico Argentino, Salta, Tomo I:391–392

Isacks B (1988) Uplift of the central Andean plateau and bending of the Bolivian orocline. J Geophys Res 93:3211–3231

Llambias EJ, Sato AM, Tomsic S (1985) Geologia y caracteristicas quimicas del stock terciario del Nevado de Arcay y vulcanitas asociadas, Provincia de Salta. Asociación Geológica Argentina 40(3–4):158–175

Lindsay JM, de Silva S, Trumbull R, Emmermann R, Wemmer K (1999) La Pacana caldera, N. Chile: a re-evaluation of the stratigraphy and volcanology of one of the world's largest resurgent calderas. J Volcanol Geotherm Res 106:145–173

Lipman PW (1997) Subsidence of ash-flow calderas: relation to caldera size and magma-chamber geometry. Bull Volcanol 59:198–218

Wernicke B, Burchfiel BC (1982) Modes of extensional tectonics. J Struct Geol 4:105–115

Marrett RA, Allmendinger RW, Alonso RN, Drake RE (1994) Late Cenozoic tectonic evolution of the Puna Plateau and adjacent foreland, northwestern Argentine Andes. J South Am Earth Sci 7:179–207

Moore ID, Kokelaar P (1997) Tectonic influences in piecemeal caldera collapse at Glencoe Volcano, Scotland. J Geol Soc Lond 154(5):765–768

Moore I, Kokelaar P (1998) Tectonically controlled piecemeal caldera collapse: a case study of Glencoe volcano, Scotland. Geol Soc Am Bull 110(11):1448–1466

Moreno JA (1970) Estratigrafía y paleogeografía del Cretácico superior en la cuenca del noroeste argentino, con especial mención de los Subgrupos Balbuena y Santa Bárbara. Asociación Geológica Argentina 25(1):9–44

Petrinovic IA, Mitjavila J, Viramonte JG, Marti J, Becchio R, Arnosio JM, Colombo F (1999) Descripción geoquímica y geochronológica de secuencias volcánicas neógenas de Trasarco, en el extremo oriental de la Cadena Volcánica Transversal del Quevar (Noroeste de Argentina). In: Colombo F, Queralt I, Petrinovic I (eds) Geológia de los Andes Centrales Meridionales: El noroeste Argentino. Acta Geológica Hispánica 34:255–272

Petrinovic IA, Riller U, Brod JA (2005) The Negra Muerta Volcanic Complex, southern central Andes: geochemical characteristics and magmatic evolution of an episodically active volcanic centre. J Volcanol Geotherm Res 140:295–320

Reyes FC, Salfity JA (1973) Cosideraciones sobre la estratigrafía del Cretácico (Subgrupo Pirgua) del noroeste Argentino. V. Congreso Geológico Argentino, Actas III:355–385

Richards JP, Villeneuve M (2002) Characteristics of late Cenozoic volcanism along the Archibarca lineament from Cerro Llullaillaco to Corrida de Cori, northwest Argentina. J Volcanol Geotherm Res 116:161–200

Riller U, Oncken O (2003) Growth of the Central Andean plateau by tectonic segmentation is controlled by the gradient in crustal shortening. J Geol 111:367–384

Riller U, Petrinovic I, Ramelow J, Strecker M, Oncken O (2001) Late Cenozoic tectonism, collapse caldera and plateau formation in the central Andes. Earth Plant Sci Lett 188:299–311

Riller U, Greskowiak J, Ramelow J, Strecker M (1999) Dominant modes of Andean deformation in the Calchaquí River Valley, NW-Argentina, XIV. Congreso Geológico Argentino, Actas I:201–204

Salfity JA., Marquillas, RA (1994) Tectonic and sedimentary evolution of the cretaceous-Eocene Salta Group Basin, Argentina. In: Salfity JA (ed) Cretaceous Tectonics of the Andes, Earth Evolution Sciences, pp 266–315

Schurr B, Asch G, Rietbrock A, Kind R, Pardo M, Heit B, Monfret T (1999) Seismic and average velocities beneath the Argentine Puna Plateau. Geophys Res Lett 26:3025–3028

Servicio Geológico Minero Argentina (1996) Hoja Geologica 2566-I (scale 1: 250.000), San Antonio de Los Cobres, Provincias de Jujuy y Salta, Republica Argentina. Boletin 217:126

Turner FJ (1953) Nature and dynamic interpretation of deformation lamellae in calcite and three marbles. Am J Sci 251:276–298

Turner JCM (1959) Estratigrafía del cordón de Escaya y de la Sierra de la Rinconada, Jujuy. Asociacion Geológica Argentina 15:16–39

Ventura G (1994) Tectonics, structural evolution and caldera formation on Volcano Island (Aeolian Archipelago, southern Thyrrhenian Sea). J Volcanol Geotherm Res 60:207–224

Vilela CR (1951) Acerca del hallazgo del horizonte calcáreo dolomítico en la Puna Salto-jujeña y su significado geológico. Asociacion Geológica Argentina 6(2):101–107

Viramonte JG, Omarini RH, Araña Saavedra V, Aparicio A, García Cacho L, Parica P (1984) Edad, genesis y mecanismos de erupcion de las riolitas granatiferas de San Antonio de los Cobres, Provincia de Salta, IX. Congreso Geológico Argentino. Actas III:216–233

Viramonte JG, Petrinovic IA (1990) Cryptic and partially buried calderas along a strike- slip fault system in the Central Andes. Int Symp on Andean Geodynamics, Grenoble. Actas I:318–320

Walker GPL (1984) Downsag calderas, ring faults, caldera sizes and incremental caldera growth. J Geophys Res 89:8407–8416